# A glimpse into the coronary applications of optical coherence tomography

## *Optyczna tomografia koherentna. Zastosowanie w kardiologii interwencyjnej*

Paweł Tyczyński[1, 2], Adam Witkowski[1], Neville Kukreja[2], Peter Barlis[3], Elio Pieri[2], Carlo Di Mario[2, 4]

[1] Institute of Cardiology, Warsaw, Poland
[2] The Royal Brompton Hospital, London, United Kingdom
[3] The Northern Hospital, Melbourne, Australia
[4] Imperial College, London, United Kingdom

Post Kardiol Interw 2009; 5, 3 (17): 148–157

**Key words:** optical coherence tomography, percutaneous coronary intervention

**Słowa kluczowe:** optyczna tomografia koherentna, przezskórna interwencja wieńcowa

### Principles and safety of optical coherence tomography

Optical coherence tomography (OCT) is an optical analogue of intravascular ultrasound (IVUS), measuring the back-reflection of infrared light from biological micro-structures (fig. 1). The axial OCT resolution is 10-20 μm what is approximately 10 times higher than that offered by IVUS. The imaging depth of only 1.0-1.5 mm within the coronary artery wall is mainly limited by the tissue attenuation of the infrared light. Near microscopic OCT resolution allows a very accurate visualization of superficial vessel wall structures and provides insight into the interaction between vessel wall and implanted stents [1].

Safety and feasibility of both IVUS and OCT (using exclusively occlusive technique in the latter) was addressed in the study of 76 patients by Yamaguchi et al. Although, transient chest pain and ischemic ECG changes during OCT image acquisition were not part of the study, they did not report any significant adverse events including vessel dissection or fatal arrhythmia [2]. Still, a number of potentially dangerous risks needs to be considered. Kim et al. reported thrombus formation during OCT imaging which highlights the need for careful systemic anticoagulation with activated clotting time (ACT) control [3]. In the LEADERS trial OCT sub-study ventricular fibrillation (VF) in one patient was induced by contrast flushing [4]. Finally, a retrospective multicenter registry was carried out to assess OCT safety in 468 patients. Of note, only 43.5% of these cases were performed using a non-occlusive OCT acquisition technique. Transient chest pain and QRS complex widening/ST segment depression/elevation were observed in nearly half of all cases. Major complications included five (1.1%) cases of ventricular fibrillation due to balloon occlusion and/or deep guide catheter intubation, 3 (0.6%) cases of air embolism and one case of vessel dissection (0.2%) [5]. To minimize the possibility of VF during non-occlusive OCT imaging iso-osmolar contrast is recommended. Its main advantage over other contrast agents lies in its higher viscosity, which permits optimal blood clearance during OCT imaging at a given flush volumes [6].

### Technique of image acquisition

Currently, OCT image acquisition is performed using commercially available systems: M2, M3 (time-domain) or C7 (optical frequency domain imaging- OFDI; synonym: swept source- SSOCT or M4) (LightLab Imaging Inc. Westford, MA, USA) with pullback speed of 2, 3 and 20 mm/s (M2, M3 and C7 models, respectively). Other companies are also developing OCT technology (e.g. Volcano Corp., USA). Following administration of intravenous heparin or bivalirudin and nitrates, an end-hole microcatheter (e. g. 0.021" Transit™, Cordis Neurovascular, Miami Lakes, FL, USA) is advanced distally to the site of interest over conventional guide wire, which is then replaced by the imaging wire (maximum outer diameter of 0.019"). The latest C7 imaging wire is integrated in a rapid-exchange catheter, that can be

**Adres do korespondencji/*Corresponding author:*** Prof. Carlo Di Mario MD, PhD, Consultant Cardiologist, The Royal Brompton Hospital, Sydney Street, London SW3 3NP, tel.: +44 207 351 86 16, fax: +44 207 351 81 04, e-mail: C.DiMario@rbht.nhs.uk or Paweł Tyczyński, e-mail: medykpol @wp.pl
Praca wpłynęła 12.08.2009, przyjęta do druku 19.08.2009.
Dr Paweł Tyczyński is the recipient of the training fellowship 2008 of the European Association of Percutaneous Coronary Interventions (EAPCI).

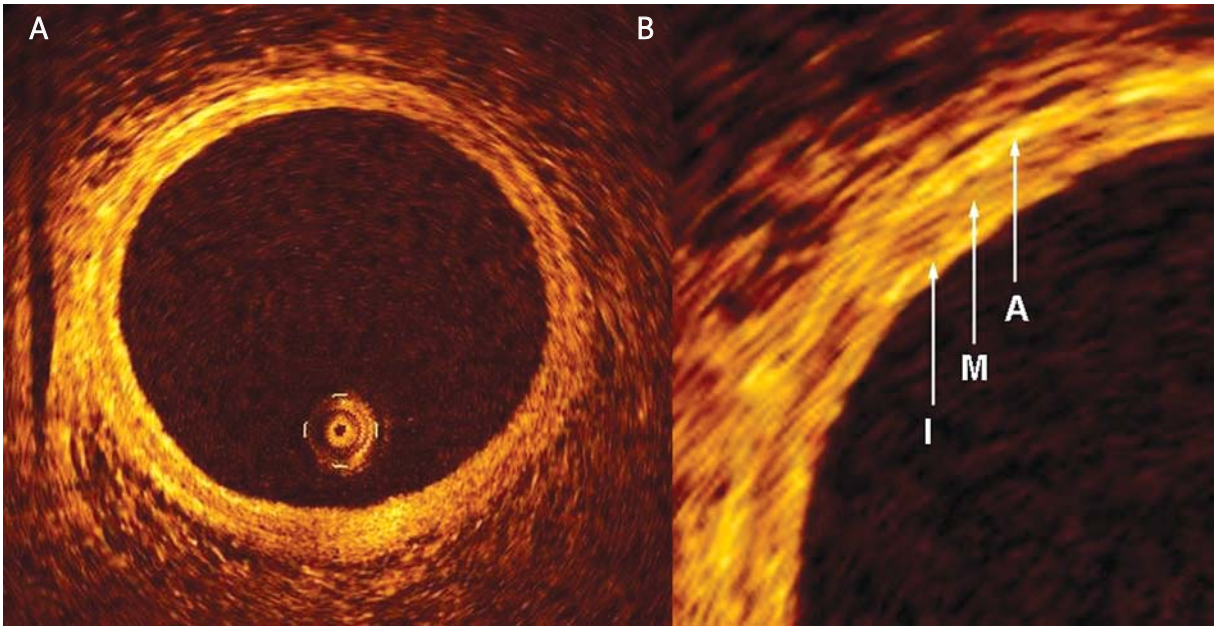


**Fig. 1. A** – OCT cross-section within normal coronary artery, **B** – magnification of image 'A' showing three layers of the coronary artery wall: I – intima, M – media, A – adventitia

***Ryc. 1. A** – przekrój poprzeczny w OCT prawidłowego segmentu tętnicy wieńcowej, **B** – powiększenie obrazu „A" pokazujące trzy warstwy ściany tętnicy wieńcowej: I – błona wewnętrzna, M – błona środkowa, A – przydanka*

delivered over a conventional guide wire without use of microcatheter. As blood cells are opaque to infrared light, continuous contrast flushing of the artery during image acquisition is required using preferably a non-occlusive technique [7]. The flushing speed via an automated injector should be adjusted to the body weight and coronary artery size, usually ranging between 2-5 ml/s.

## Optical coherence tomography image analysis

Off-line image analysis allows careful assessment of the acquired images. Post-intervention OCT evaluation of implanted stents allows precise insight into stent strut apposition and quantification of malapposed struts. There is no unified methodology regarding analyzed intervals for assessment of both strut apposition and strut tissue coverage at follow-up: previous authors have actually used 1000 μm intervals (Chen et al., Katoh et al., Takano at al., Barlis et al.). In sites of special interest, like bifurcations, smaller intervals (500 μm) should be considered. Indeed, in ODESSA trial the analyzed intervals were of 300 μm [8]. Consensus is currently being worked on with an international collaboration of OCT users.

## Clinical applications

### Optical coherence tomography guidance during percutaneous coronary intervention

Similarly to IVUS, OCT is reliable tool to accurately measure the lumen area and diameter [an essential measurement to select a device with a limited range of expansion like pericardium covered stents to treat very degenerated saphenous vein graft (SVG) lesions] [9]. Taking into account a smaller OCT scan area (7-8 mm for M3 model and 12-13 mm for C7 model), than that one offered by IVUS, OCT is not very suitable for large vessels like SVG or carotids (fig. 2).

### Coronary stents

Since the metallic surface of the strut is opaque to infrared light, the abluminal strut surface cannot be seen; therefore stent struts were defined as malapposed if the distance between the endoluminal surface of the strut and the vessel wall was greater than the thickness of the strut (metal + polymer).

### Immediate results after stenting

Stent apposition immediately after its implantation is of paramount importance since it can influence healing process. Malapposed struts of the stent might have less chance of being covered by neointima. An IVUS study by Cook et al. showed that in patients who developed late stent thrombosis, incomplete stent apposition was more frequent than in the control group (77 vs. 12% respectively, $p < 0.001$) [10]. Many factors like anatomy, clinical presentation during percutaneous coronary intervention (PCI), and technical aspects of PCI (stent type, technique) influenced immediate stent apposition.

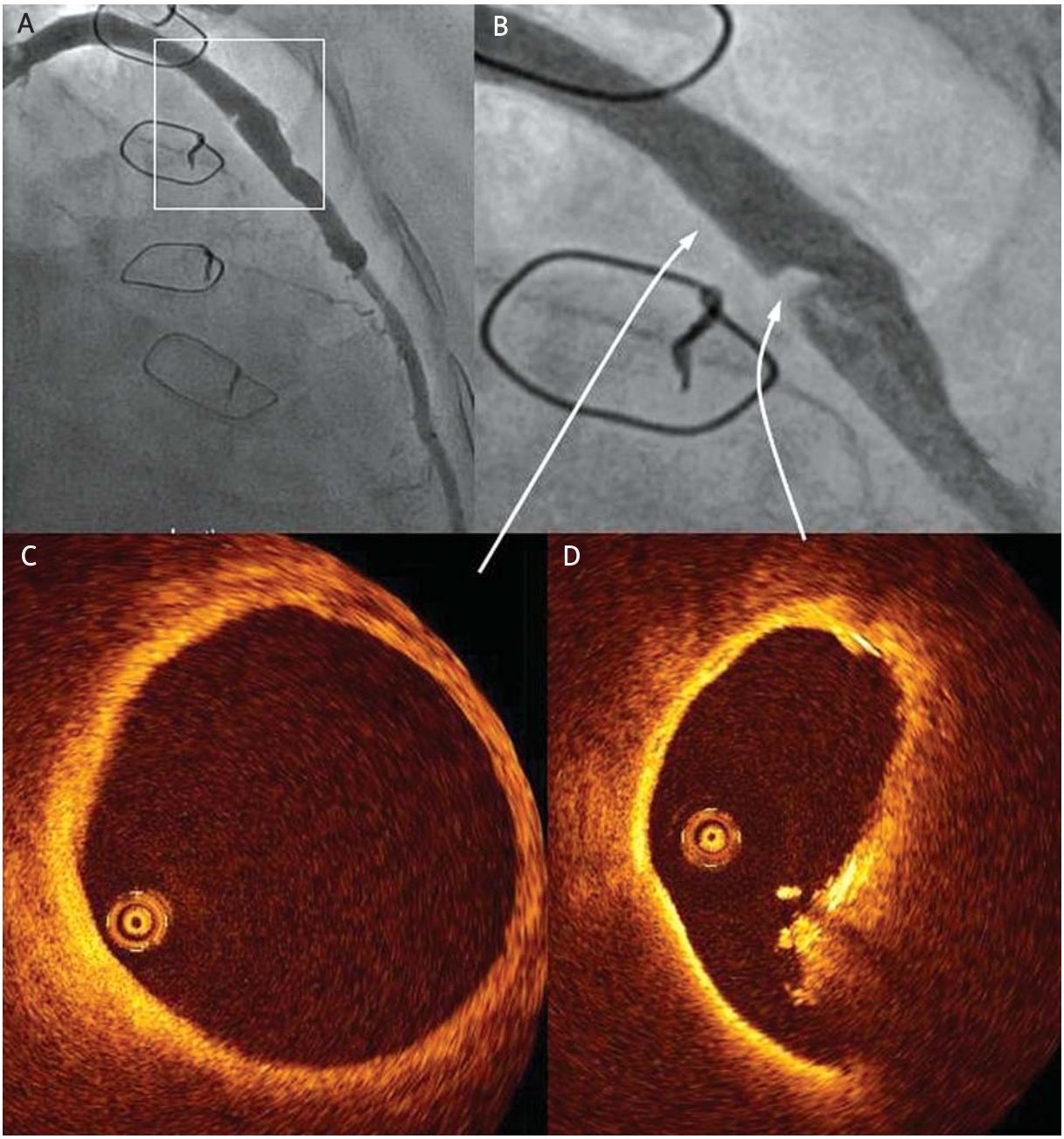


**Fig. 2. A** – angiogram showing degenerated SVG, **B** – magnification of image 'A' showing short, irregular and borderline stenosis in the mid portion of the SVG, **C, D** – corresponding OCT images showing almost normal segment of the SVG and stenosis with very irregular borders

***Ryc. 2. A** – zdegenerowany pomost żylny w angiografii, **B** – powiększenie obrazu „A" pokazujące krótkie, nieregularne i graniczne zwężenie w środkowym segmencie pomostu, **C, D** – odpowiadające (strzałki) przekroje poprzeczne w OCT pokazujące niemal prawidłowy segment pomostu żylnego oraz zwężenie z bardzo nieregularnym zarysem*

### *Straight segments*

In a study of 23 patients Tanigawa at al. showed that stent strut malapposition may persist despite angiographic optimization with oversized post-dilatation using high pressure balloons. The strut malapposition rate was 9.1 ± 7.4% and the sirolimus-eluting stent (SES) was characterized by significantly higher malappostion rate than paclitaxel-eluting stent (PES) (11.6 ± 6.6% vs. 3.7 ± 5.2%, p = 0.007), possibly as a result of a thicker strut profile and closed cell design [11].

### *Overlapping segments*

As expected, segments where stents overlap are characterized by higher malapposition rates. Indeed, in

a small study of 10 patients, OCT showed that 41.8 ± 21.5% of struts were not apposed to the vessel wall, compared to less than the half malapposition rate in the proximal and distal segments [12].

### *Bifurcation lesions*

Non-uniform 3D geometry of bifurcation lesion makes it difficult to achieve well apposed stent struts to the vessel wall at the take-off of the side branch. Higher stent thrombosis rate after bifurcation PCI than in straight segments is linked not only to non-uniform blood flow but with high probability also to delayed healing due to higher stent malapposition in this area [13]. Previous IVUS studies deliberately excluded these segments from further analyses due to prominent artifacts generated by this technique [14] and they have focused on poor expansion rather malapposition. In an IVUS study by Costa et al. more than 60% of cases after 'crush' were found to have stent malapposition [15]. Our preliminary OCT results indicate that the prevalence of malapposed struts in bifurcation lesions treated with different one- and two-stents techniques may be significantly higher at the level of the bifurcation (almost 30%) than in the proximal and distal segments. The highest percent of malapposed struts was observed in the 2 quadrants toward the side branch (> 40%) (fig. 3).

### *Clinical presentation*

Drug eluting stent (DES) thrombosis is largely determined by the clinical setting and acute coronary syndrome (ACS) at presentation was found to be an independent predictors of DES thrombosis [16]. The possible explanation of this unfavorable outcome is worse stent apposition seen after PCI in the setting of ACS.

### Detection of vessel injury after stenting

High resolution of OCT allows easy and accurate insight into two most common injuries after stent implantation: edge dissection and plaque prolapse (fig. 4).

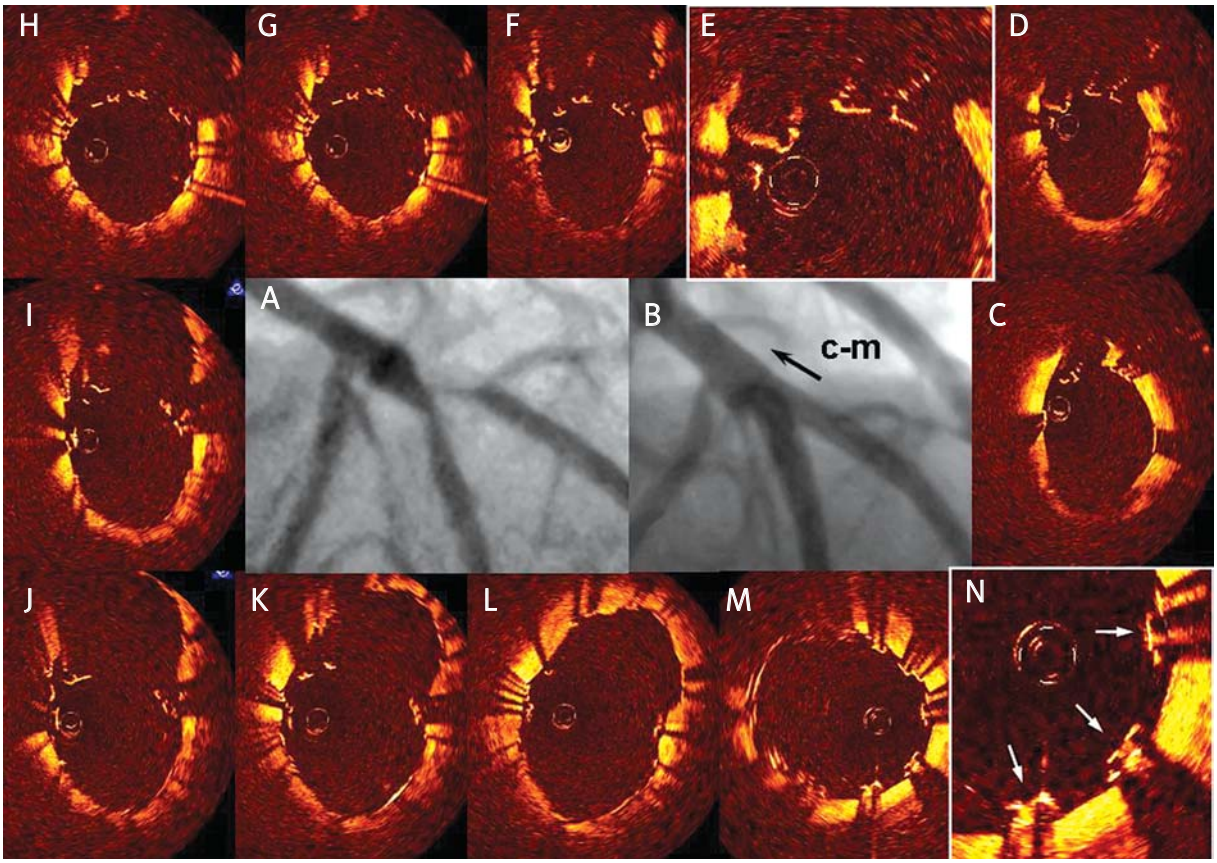


**Fig. 3. A** – bifurcation lesion involving LAD and Dg, **B** – final angiographic result after implantation of two stents into LAD and Dg (Culotte technique), **C-D** and **F-M** – OCT images in the bifurcation showing malapposed/floating struts in the half facing the SB, **E** – magnification of the image '**D**' focused on malapposed struts, **N** – magnification of the image 'M' showing well apposed two layers of struts in the proximal segment

***Ryc. 3. A** – zmiana w rozwidleniu LAD i Dg, **B** – końcowy wynik angiograficzny po implantacji dwóch stentów do LAD oraz Dg (technika Culotte), **C–D** oraz **F–M** – przekroje rozwidlenia w OCT pokazujące nieprzylegające struty stentu, które znajdują się naprzeciw ujścia gałęzi bocznej, **E** – powiększenie obrazu „D" pokazujące nieprzylegające struty stentu, **N** – powiększenie obrazu „M" pokazujące dobrze przylegające dwie warstwy strutów w segmencie proksymalnym tętnicy*

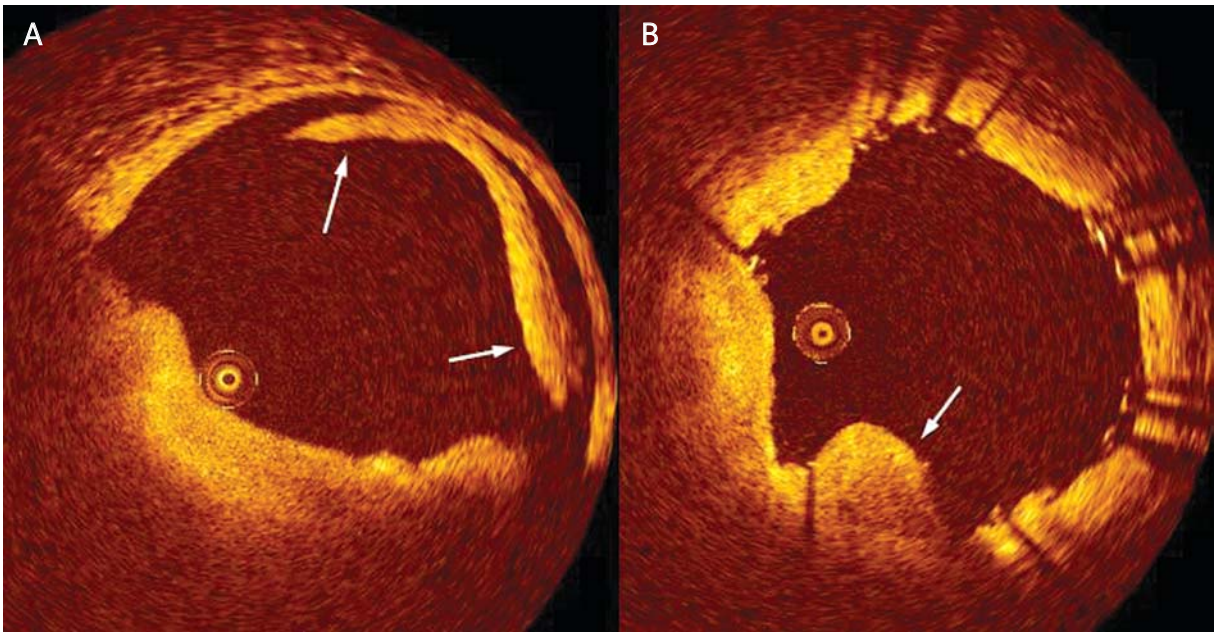


**Fig. 4. A** – edge dissection after implantation of stent (arrows), **B** – plaque prolapse through stent struts (arrow)
***Ryc. 4. A** – dysekcja (rozwarstwienie) na krawędzi stentu po jego implantacji (strzałki), **B** – prolaps blaszki poprzez struty stentu (strzałka)*

IVUS observations suggested that substantial dissections following PCI, which do not diminish antegrade blood flow, do not lead to an increase in acute or long-term events [17]. However, another IVUS study showed that the area stenosis at the site of non-obstructive dissections was a predictor of acute vessel closure [18]. There is lack of clinical relevance of OCT detected edge dissection. Plaque prolapse can potentially lead to distal embolization, but previous IVUS study following PCI in diabetic patients did not give evidence of its detrimental role [19]. There are not yet available OCT data regarding this phenomenon.

## Follow-up observations

The issue of stent coverage by neointima is particularly pertinent given that autopsy series have identified a strong link between incomplete endothelialization and stent thrombosis. In a post-mortem study by Finn et al. the most powerful histological predictor of stent thrombosis was endothelial coverage and a ratio of uncovered to total stent struts per section > 30% had an odds ratio for stent thrombosis of 9 (95% CI 3.5-22) [20]. Of particular interest are complex lesions like bifurcations and long lesions requiring overlapping stents. Current clinical experience demonstrates the high level of accuracy of OCT in evaluating the heterogeneity of vascular healing following DES implantation [21]. Two OCT parameters are usually assessed at OCT follow-up: stent coverage and stent apposition. Additionally neointimal hyperplasia (NIH) measurement was included into analyses in some trials. Given the aforementioned superiority in resolution between IVUS and OCT, the latter one is much more precise to accurately quantify tissue coverage. Unlike bare metal stents (BMS) which develop stent coverage with an average thickness of 500 μm or more, which is sufficient enough to be detected by IVUS, DES coverage is frequently far below this IVUS resolution (fig. 5 and 6). Indeed, the distribution of neointimal thickness across all struts in the LEADERS OCT sub-study (biolimus eluting stent with biodegradable polimer vs. SES) showed that for 67% of all struts neointimal thickness was < 100 μm, the resolution of IVUS [4]. Similar results were reported by Matsumoto et al. [22].

Several anatomical, clinical, procedural factors and stent design might potentially influence the healing process after stent implantation. Table 1 summarizes the OCT studies done so far for assessment of stent coverage by neointima. The rate of uncovered struts ranged between 0.02% for Zotarolimus eluting stent – ZES (Endeavor, Medtronic, USA) 6 months after DES implantation (ODESSA trial) and 15.2% for SES (Cypher, Cordis, USA) 8.6 months after implantation in the study by Chen et al. [23].

The prospective, randomized, multicenter ODESSA trial aimed to compare stent coverage between overlapping and non-overlapping segments in four different types of stents [7]. At 6 month OCT follow-up there were no

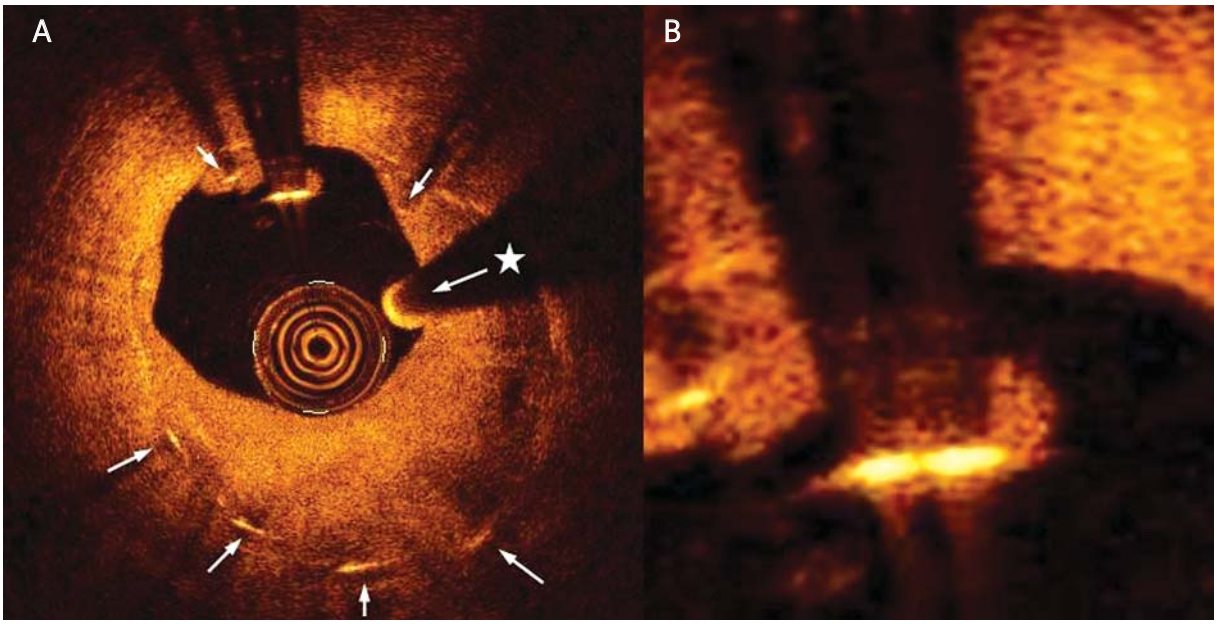


**Fig. 5. A** – OFDI image – non-homogenous DES neointimal coverage 9 months after its implantation. Neointimal hyperplasia is visible at 3-7 o'clock and very thin coverage of malapposed strut at 12 o'clock (arrows – shadows of struts; asterisk – shadow of guidewire), **B** – magnification of image 'A' showing single malapposed strut

***Ryc. 5. A** – obraz OFDI – niehomogenne pokrycie stentu typu DES przez neointimę po 9 miesiącach od jego implantacji. Na godzinie 3.–7. widoczny jest nadmierny przerost neointimy, natomiast na godzinie 12. bardzo cienkie pokrycie stentu przez neointimę (strzałki – cienie strutów; gwiazdka – cień prowadnika), **B** – powiększenie obrazu „A" pokazujące pojedynczy, nieprzylegający strut*

**Table 1.** Optical coherence tomography trials assessing the ratio of uncovered struts among different stent types and at different follow-up duration

***Tabela 1.** Brak pokrycia strutów stentów w obserwacji odległej. Ocena za pomocą optycznej tomografii koherentnej*

| Study | Type of stent | No of patients [n] | Follow-up duration [months] | Ratio of uncovered struts [%] |
|---|---|---|---|---|
| LEADERS | Cypher | 22 | 9 | 2.1 |
| | Biomatrix | 20 | 9 | 0.6 |
| HORIZONS-AMI | Express BMS | 29 | 13 | 0.9 |
| | Taxus | 88 | 13 | 4.8 |
| ODESSA | Cypher | 22 | 6 | 5.8 |
| | Taxus | 22 | 6 | 2.7 |
| | Endeavor | 22 | 6 | 0.02 |
| | Liberte BMS | 20 | 6 | 1.8 |
| ATLANTA | CATANIA stent | 15 | 6 | 0.5 |
| Matsumoto et al. | Cypher | 34 | 6 | 11 |
| Takano et al. 1 | Cypher | 21 | 3 | 15 |
| Takano et al. 2 | Cypher | 21 | 24 | 5 |
| Chen et al. | BMS | 7 | 7.3 | 0.3 |
| | BMS | 6 | 44 | 0.3 |
| | Cypher | 10 | 8.6 | 15.2 |
| Tian et al. | Cypher-overlap | 22 | 12 | 12.6 |
| Kim et al. | Endeavor | 32 | 9 | 0.3 |
| | Cypher | 36 | 9 | 12.2 |

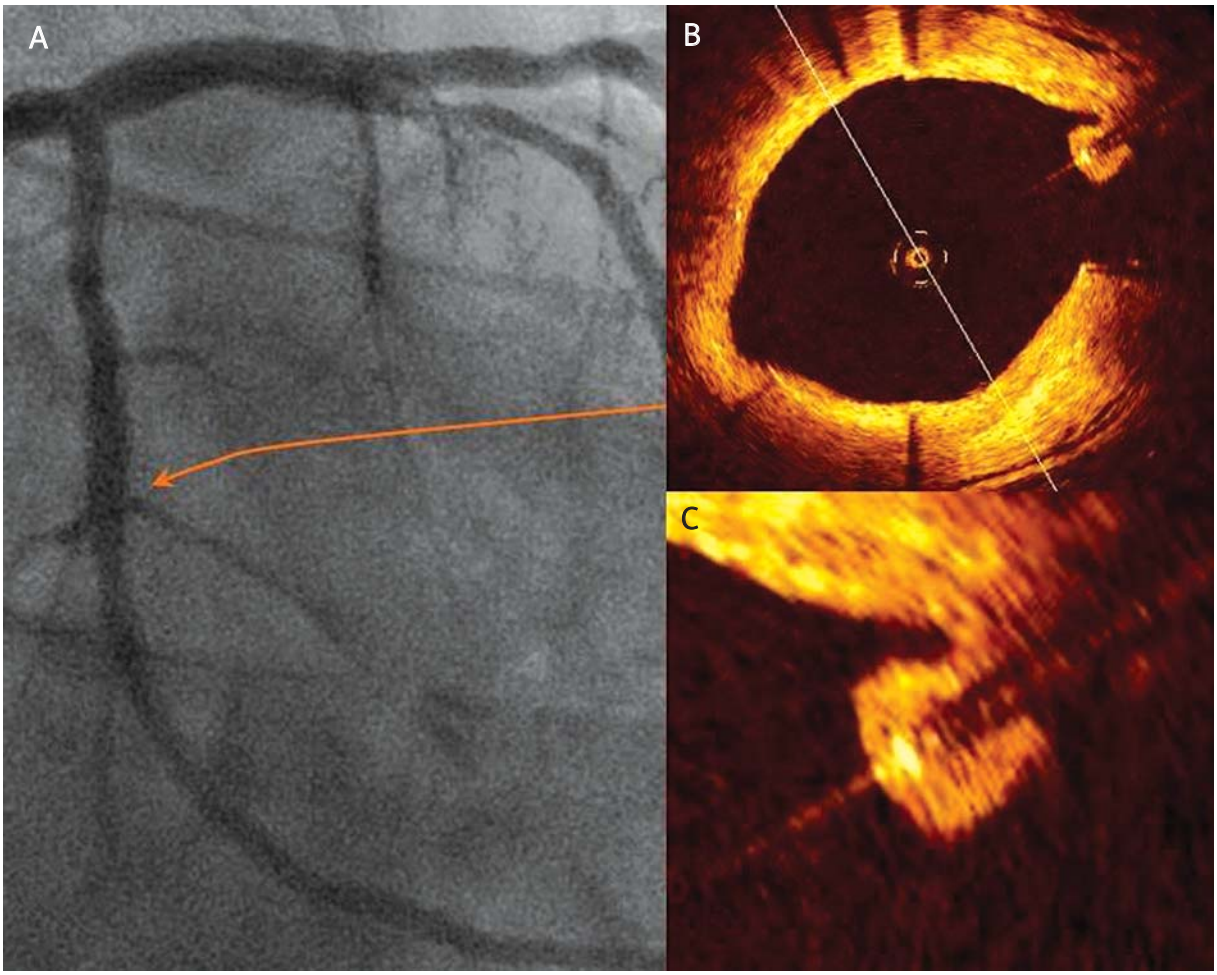


**Fig. 6. A** – angiography of LCx 11 months after DES implantation, **B** – OCT image showing well apposed struts and one malapposed, covered strut at the site of SB take-off

***Ryc. 6. A** – angiografia LCx po 11 miesiącach od implantacji DES, **B** – obraz OCT pokazujący dobrze przylegające stenty oraz jeden z nich, znajdujący się w miejscu odejścia gałęzi bocznej – nieprzylegający, pokryty przez neointimę*

observed significant differences in both stent coverage and strut malapposition between overlapping and non-overlapping segments (2.7 and 2.6 vs. 2.3 and 0.8%, $p = 0.76$, respectively). Stent types differed and SES and PES (Taxus, Boston Scientific, USA) were characterized by the highest rate of uncovered struts (5.8% and 2.7%, respectively). Additionally, these two stents had the highest rate of strut malappostion (2.9% and 5.5%, respectively), as compared to only 0.04% of malapposed struts of ZES.

Durable polymer surface coating may contribute for delayed endothelialization of first generation of DES. The aforementioned LEADERS (Limus Eluted from A Durable versus ERodable coating) study, was a multi-center, randomized non-inferiority trial comparing a biolimus-eluting stent (BES), with a biodegradable polymer and SES with durable polymer. An OCT sub-study which was a superiority study, enrolled 20 patients in BES group and 26 patients in SES group. It revealed 3 lesions in BES and 15 lesions in SES with ≥ 5% of all uncovered struts ($p < 0.01$) [4].

The single-center OCT sub-study of HORIZONS AMI trial enrolled STEMI patients treated with either Express BMS or PES (3 : 1). At 13 month OCT follow-up > 90% of struts were covered by neointima, but there was observed significant difference in both stent coverage and malappostion rate in favour of BMS (0.9 and 0.1 vs. 4.8 and 1.2%, $p < 0.001$ and $p = 0.003$ respectively) [24].

Healing of bifurcation lesions is of particular interest given the higher thrombosis rate in this region as compared to straight segments [25]. Taking into account higher incidence of malapposed struts at the bifurcation level [26], mainly caused by the creation of the metallic neo-carina (fig. 3), the healing process might be hindered (fig. 7). An OCT study by Katoh et al., which included both straight segments and bifurcation sites in 13 patients showed improvement in intimal coverage between

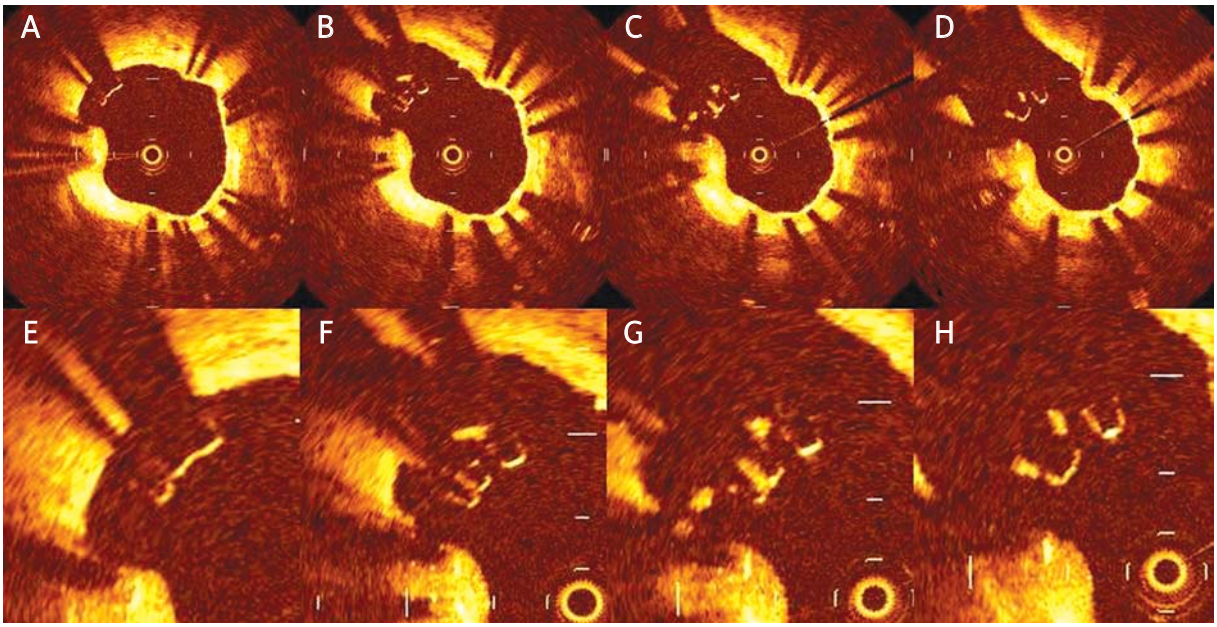


**Fig. 7. A-D** – consecutive OCT images showing DES 9 months after implantation. Most of well apposed struts are covered by thin layer of neoinima, but malapposed struts protruding into the SB take-off are still uncovered, **E-H** – magnifications of images 'A-D' focused on malapposed and uncovered struts

***Ryc. 7. A–D*** *– kolejne przekroje OCT pokazujące DES po 9 miesiącach od implantacji. Większość dobrze przylegających strutów stentu jest pokryta przez neointimę, natomiast struty nieprzylegajace, znajdujące się w miejscu odejścia gałęzi bocznej, pozostają ciągle niepokryte,* ***E–H*** *– powiększenie obrazów „A–D" – struty nieprzylegające i niepokryte przez neointimę*

6 months and 12 months after implantation of SES. Interestingly, they found that the frequency of struts located at the SB orifice without neointima decreased from 4 out of 17 (24%) at 6 months to 0 out of 17 (0%) at 12 months of follow-up [27].

Finally the clinical presentation of patients at initial procedure could potentially influence the rate of strut coverage at follow-up as a result of differences in stent apposition during initial procedure [28]. In a study by Gonzalo et al. forty-seven lesions in 43 patients (49% stable angina, 17% unstable angina, 34% STEMI) were assessed by OCT at a median follow-up time of 9 months. Frequency of uncovered struts was also higher in the STEMI group than in stable angina/unstable angina group (93.8 vs. 67.7% respectively, p = 0.048). DES implantation in STEMI was the only independent predictor of ISA (OR 9.8, 95% CI 2.4-40.4, p = 0.002) and the presence of uncovered struts at follow-up (OR 9.5, 95% CI 1.0-90.3, p = 0.049) [29].

### Plaque assessment

Several studies were conducted to demonstrate the utility of OCT in characterizing atherosclerotic plaques. Detailed description of these trials is beyond this review. Briefly, when compared with histological specimens from autopsy, the initial studies reported the sensitivity and specificity ranged from 71% to 79% and 97% to 98% for fibrous plaques, 95% to 96% and 97% for fibrocalcific plaques, and 90% to 94% and 90% to 92% for lipid-rich plaques, respectively [30]. However, a recent observations by Manfrini et al. indicated that plaque misclassification may occur even in more than 40%, predominantly due to limited OCT signal penetration, which could hamper detection of lipid pools or calcium behind thick fibrous caps, and by an inability to distinguish calcium deposits from lipid pools or the opposite [31]. Indeed OCT is able to measure precisely the fibrous cap thickness, but not necessarily deeper lying plaque components (fig. 8). Combined use of OCT with virtual histology IVUS (VH-IVUS) can potentially overcome these limitations, especially in identifying vulnerable plaques [32]. Previous IVUS studies (REVERSAL, ASTEROID) suggested that intensive lipid lowering therapy might result in regression of atherosclerosis. Additionally, OCT demonstrated that in patients after ACS, statins can definitely increase the thickness of the fibrous cap overlying vulnerable non-culprit plaque [33].

## Optical coherence tomography limitations

Continuous intracoronary OCT imaging is not possible unless blood is cleared from the artery. This makes the OCT technique difficult for real-time PCI guidance, e.g. for positioning of the wire in advanced PCI techniques like those dedicated for chronic total occlusion (CTO). Still, in selected cases, it can be helpful in challenging cases like stumpless CTO's where it can show exactly

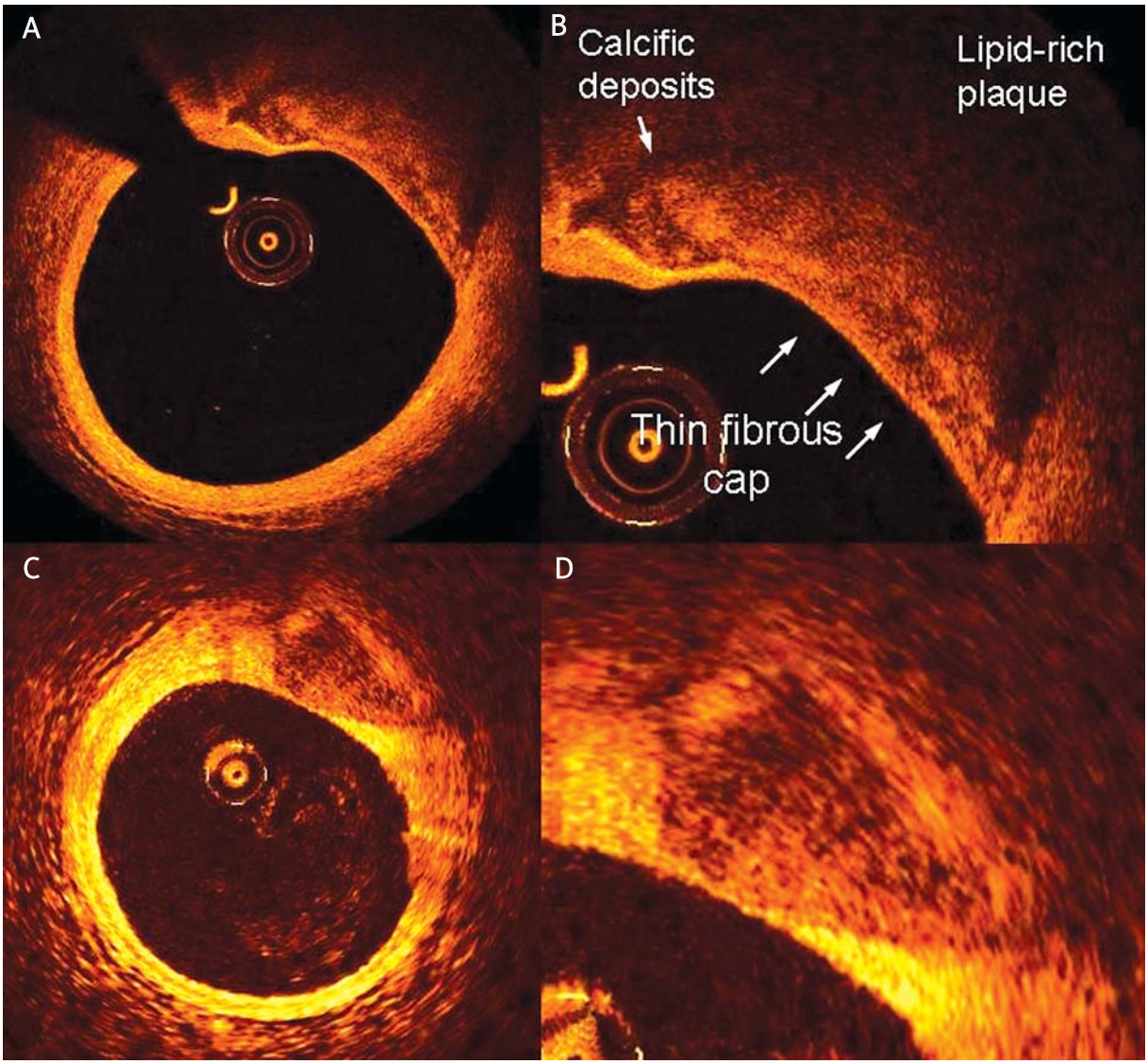


**Fig. 8.** Two different types of atherosclerotic plaques in OCT, both covered by thin fibrous cap (< 60 μm): **A** – lipid-rich plaque with non-defined outer borders and few calcific deposits (left shoulder), **B** – magnification of image „A", **C** – fibro-calcific plaque with well-defined outer borders, **D** – magnification of image „C"

***Ryc. 8.*** *OCT – dwa różne typy blaszki miażdżycowej, pokrytej cienką otoczką włóknistą (< 60 μm): **A** – blaszka o dużej zawartości lipidów ze źle odgraniczonym zarysem zewnętrznym i nielicznymi depozytami wapniowymi (lewe ramię), **B** – powiększenie obrazu „A", **C** – blaszka włóknista z obecnością zwapnień z dobrze odgraniczonym zarysem zewnętrznym, **D** – powiększenie obrazu „C"*

the entry point and confirm correct positioning of a stiff guide wire [34]. OCT trials performed so far enrolled quite modest number of patients. The amount of work required for quantitative analysis of neointimal thickness, strut coverage and stent apposition is potentially discouraging clinical trials from enrolling high number of patients (e. g. the number of struts evaluated in ODESSA trial was 53047). The OCT analysis must be simplified, standardized and preferably automated [35]. The results from OCT follow-up after stent implantation must be interpreted with caution as OCT still does not have endothelial cell resolution neither provides functional tissue differentiation. Finally, OCT couldn't really tell what types of cells are covering the struts: they might be fibrin and not endothelium.

## Future developments

Computer assisted detection of stent malapposition or neointimal coverage is being explored. Such software could enable faster evaluation of large number of struts.

Integration of VH-IVUS into OCT software might give additional assessment of plaque morphology. Further OCT development of functional imaging in the direction of plaque characterisation (polarisation OCT), vasa vasorum/intraplaque haemorrhage and ligands (e.g. plaque inflammation, adhesion molecules) is needed. Three-dimensional reconstruction and assessment of OCT images is being developed.

## References


1. Low AF, Tearney GJ, Bouma BE, Jang IK. Technology insight: optical coherence tomography-current status and future development. Nat Clin Pract Cardiovasc Med 2006; 3: 154-162.
2. Yamaguchi T, Terashima M, Akasaka T, et al. Safety and feasibility of an intravascular optical coherence tomography image wire system in the clinical setting. Am J Cardiol 2008; 101: 562-567.
3. Kim JS, Kim JS, Choi EY, et al. Images in cardiovascular medicine. Catastrophic thrombus formation during optical coherence tomography. Circulation 2008; 118: e101-102.
4. Barlis P, Regar E, Serruys PW, et al. An Optical Coherence Tomography Study of a Biodegradable versus Durable Polymer-Coated Limus-Eluting Stent: A LEADERS Trial Sub-Study. Eur Heart J [under revision].
5. Barlis P, Gonzalo N, Di Mario C, et al. A multicentre evaluation of the safety of intracoronary optical coherence tomography. EuroIntervention 2009; 5: 90-95.
6. Barlis P, van Soest G, Serruys PW, Regar E. Intracoronary optical coherence tomography and the evaluation of stents. Expert Rev Med Devices 2009; 6: 157-167.
7. Kataiwa H, Tanaka A, Kitabata H, et al. Safety and usefulness of non-occlusion image acquisition technique for optical coherence tomography. Circ J 2008; 72: 1536-1537.
8. Guagliumi G. ODESSA trial. Transcatheter Cardiovascular Therapeutics, Washington DC 2008.
9. Tyczyński P, Kukreja N, Van Geuns RJ, et al. Optical Coherence Tomography for the assessment of pericardium covered stents for the treatment of degenerated saphenous vein grafts. EuroIntervention [under revision].
10. Cook S, Wenaweser P, Togni M, et al. Incomplete stent apposition and very late stent thrombosis after drug-eluting stent implantation. Circulation 2007; 115: 2426-2434.
11. Tanigawa J, Barlis P, Dimopoulos K, et al. The influence of strut thickness and cell design on immediate apposition of drug-eluting stents assessed by optical coherence tomography. Int J Cardiol 2009; 134: 180-188.
12. Tanigawa J, Barlis P, Dimopoulos K, Di Mario C. Optical coherence tomography to assess malapposition in overlapping drug-eluting stents. EuroIntervention 2008; 3: 580-583.
13. Joner M, Finn AV, Farb A, Mont EK, et al. Pathology of drug-eluting stents in humans: delayed healing and late thrombotic risk. J Am Coll Cardio 2006; 48: 193-202.
14. Kimura M, Mintz GS, Carlier S, et al. Outcome after acute incomplete sirolimus-eluting stent apposition as assessed by serial intravascular ultrasound. Am J Cardiol 2006; 15: 436-442.
15. Costa RA, Mintz GS, Carlier SG, et al. Bifurcation coronary lesions treated with the 'crush' technique: an intravascular ultrasound analysis. J Am Coll Cardiol 2005; 46: 599-605.
16. Daemen J, Wenaweser P, Tsuchida K, et al. Early and late coronary stent thrombosis of sirolimus-eluting and paclitaxel-eluting stents in routine clinical practice: data from a large two-institutional cohort study. Lancet 2007; 369: 667-678.
17. Schroeder S, Baumbach A, Mahrholdt H, et al. The impact of untreated coronary dissections on acute and long-term outcome after intravascular ultrasound guided PTCA. Eur Heart J 2000; 21: 137-145.
18. Nishida T, Colombo A, Briguori C, et al. Outcome of nonobstructive residual dissections detected by intravascular ultrasound following percutaneous coronary intervention. Am J Cardiol 2002; 89: 1257-1262.
19. Futamatsu H, Sabaté M, Angiolillo DJ, et al. Characterization of plaque prolapse after drug-eluting stent implantation in diabetic patients: a three-dimensional volumetric intravascular ultrasound outcome study. J Am Coll Cardiol 2006; 48: 1139-1145.
20. Finn AV, Joner M, Nakazawa G, et al. Pathological correlates of late drug-eluting stent thrombosis: strut coverage as a marker of endothelialization. Circulation 2007; 115: 2435-2441.
21. Barlis P, Dimopoulos K, Tanigawa J, et al. Quantitative analysis of intracoronary optical coherence tomography measurements of stent strut apposition and tissue coverage. Int J Cardiol 2009 Jan 18 [Epub ahead of print].
22. Matsumoto D, Shite J, Shinke T, et al. Neointimal coverage of sirolimus-eluting stents at 6-month follow-up: evaluated by optical coherence tomography. Eur Heart J 2007; 28: 961-967.
23. Chen BX, Ma FY, Luo W, et al. Neointimal coverage of bare-metal and sirolimus-eluting stents evaluated with optical coherence tomography. Heart 2008; 94: 566-570.
24. Guagliumi G. Transcatheter Cardiovascular Therapeutics, Washington DC 2008.
25. Farb A, Burke AP, Kolodgie FD, Virmani R. Pathological mechanisms of fatal late coronary stent thrombosis in humans. Circulation 2003; 108: 1701-1706.
26. Di Mario C. www.tctmd.com.
27. Katoh H, Shite J, Shinke T, et al. Delayed neointimalization on sirolimus-eluting stents. 6-month and 12-month follow up by optical coherence tomography. Circ J 2009; 73: 1033-1037.
28. Takano M, Inami S, Jang IK, et al. Evaluation by optical coherence tomography of neointimal coverage of sirolimus-eluting stent three months after implantation. Am J Cardiol 2007; 99: 1033-1038.
29. Gonzalo N, Barlis P, Serruys PW, et al. Incomplete stent apposition and delayed tissue coverage are more frequent in drug-eluting stents implanted during primary percutaneous coronary intervention for ST-segment elevation myocardial infarction than in drug-eluting stents implanted for stable/unstable angina: insights from optical coherence tomography. JACC Cardiovasc Interv 2009; 2: 445-452.
30. Yabushita H, Bouma BE, Houser SL, et al. Characterization of human atherosclerosis by optical coherence tomography. Circulation 2002; 106: 1640-1645.
31. Manfrini O, Mont E, Leone O, et al. Sources of error and interpretation of plaque morphology by optical coherence tomography. Am J Cardiol 2006; 98: 156-159.
32. Sawada T, Shite J, Garcia-Garcia HM, et al. Feasibility of combined use of intravascular ultrasound radiofrequency data analysis and optical coherence tomography for detecting thin-cap fibroatheroma. Eur Heart J 2008; 29: 1136-1146.
33. Takarada S, Imanishi T, Kubo T, et al. Effect of statin therapy on coronary fibrous-cap thickness in patients with acute coronary syndrome: assessment by optical coherence tomography study. Atherosclerosis 2009; 202: 491-497.
34. Tyczynski P, Kukreja N, Pieri E, di Mario C. Optical frequency domain imaging guided crossing of a stumpless chronic total occlusion. Int J Cardiol 2009 Jun 26. [Epub ahead of print].
35. Mintz GS. ODESSA Critique and Clinical Perspectives. www.tctmd.com.